Article

Design Optimisation Strategies for Solid Rammed Earth Walls in Mediterranean Climates

Giada Giuffrida * , **Maurizio Detommaso *** , **Francesco Nocera** and **Rosa Caponetto**

Department of Civil Engineering and Architecture, University of Catania, Viale Andrea Doria 6,
95125 Catania, Italy; francesco.nocera@unict.it (F.N.); rcapo@dau.unict.it (R.C.)
* Correspondence: giada.giuffrida@unict.it (G.G.); maurizio.detommaso@phd.unict.it (M.D.);
Tel.: +39-095-738-2500 (G.G.)

Abstract: The renewed attention paid to raw earth construction in recent decades is linked to its undoubted sustainability, cost-effectiveness, and low embodied energy. In Italy, the use of raw earth as a construction material is limited by the lack of a technical reference standard and is penalised by the current energy legislation for its massive behaviour. Research experiences, especially transoceanic, on highly performative contemporary buildings made with natural materials show that raw earth can be used, together with different types of reinforcements, to create safe, earthquake-resistant, and thermally efficient buildings. On the basis of experimental data of an innovative fibre-reinforced rammed earth material, energy analyses are developed on a rammed earth building designed for a Mediterranean climate. The paper focuses on the influences that different design solutions, inspired by traditional bioclimatic strategies, and various optimised wall constructions have in the improvement of the energy performance of the abovementioned building. These considerations are furthermore compared with different design criteria aiming at minimising embodied carbon in base material choice, costs, and discomfort hours. Results have shown the effectiveness of using the combination of massive rammed earth walls, night cross ventilation, and overhangs for the reduction of energy demand for space cooling and the improvement of wellbeing. Finally, the parametric analysis of thermal insulation has highlighted the economic, environmental, and thermophysical optimal solutions for the rammed earth envelope.

Keywords: rammed earth construction; bioclimatic strategies; cooling load; optimisation

1. Introduction

As is well known, contemporary society has a strong dependence on the use of fossil fuels such as coal and oil, the so-called non-renewable energy sources which, according to some projections based on the energy consumption scenarios of the last thirty years, will be exhausted by 2050 [1]. This scenario is exacerbated by the generalised concern for the health of our planet, which is increasingly affected by climate change, which has been shown to be also linked to the emission of greenhouse gases into the atmosphere. The European directives today, following the international guidelines defined in the Environment and Climate Summits of the last thirty years (including the Rio Conference in 92, the Johannesburg Summit in 2002, the Rio Conference in 2012, and the last summit held in New York in 2019), aim to achieve the following objectives by 2030: a reduction of at least 40% of greenhouse gas emissions into the atmosphere (compared to 1990 levels), the achievement of the development of renewable energy sources up to 32%, and an increase in energy efficiency of 32.5% [2]. In this context, the responsibility of the construction sector in the field of energy consumption and the emission of pollutants into the atmosphere, both residential and non-residential, is quite high: the International Energy Agency indicates that it accounts for 36% of global energy demand and 39% of carbon dioxide emissions, while the annual production of solid waste, in 2016, amounted to 2.01 billion tons, of which at least 40% consists of construction material [3]. It is therefore understandable that improving the

performance of buildings is fundamental to achieve the Sustainable Development Scenario: research and technological innovation aim to reduce the energy consumption of dwellings, making their envelopes more efficient and reducing the environmental impact and the amount of waste resulting from construction and demolition processes. As is known, in Central Europe, the need to ensure effective airtightness to reduce the energy demand for winter heating has led to the definition of technological solutions capable of reducing heat loss through the envelope by means of hyper-insulated buildings. In hot climates, on the other hand, the control of air flows and ventilation, together with the bioclimatic design of buildings, can allow temperatures to be maintained close to comfort without the use of active systems, during the summer season [4]. In the same countries, the maximisation of free energy supplies (solar radiation) through technological solutions of massive storage, possibly combined with the use of glass envelopes, can significantly reduce heating costs in the winter period [4].

Therefore, it seems obvious how technological solutions that provide massive masonry, such as those in raw earth, are preferred in contexts characterised by mild climates, precisely because their high thermal mass moderates and balances the temperature and humidity inside buildings, maintaining comfort conditions in buildings, as reported by several authors [5–7]. Raw earth, as a building material, has the potential to be adopted almost everywhere and has a low environmental impact in terms of manufacturing/processing [8,9]. Moreover, it can be reused when it is not stabilised with chemical binders that cause changes in the material, therefore acquiring an infinite life cycle [10].

The study of new massive construction solutions in raw earth cannot ignore the optimisation of thermophysical performance to meet the high energy standards set by current regulations. At the same time, in national and international areas affected by telluric phenomena, the thermal performance must be combined with the ability to withstand dynamic actions to ensure an effective seismic response. After reviewing the main literature that aims to study the energetic and thermophysical behaviour of massive rammed earth envelopes, the paper examines possible design strategies for the adoption of such techniques for new sustainable buildings in countries characterised by a Mediterranean climate.

Moreover, the thermophysical characterisation of an innovative fibre-reinforced rammed earth material is presented. Then, on the basis of these experimental results, a thermal and energy analysis is implemented to simulate the thermophysical behaviour and energy needs of a rammed earth building designed for the city of Catania, Italy.

2. State of the Art on Thermal Behaviour of Massive Raw Earth Buildings

With the aim of reducing energy consumption by contemporary construction, the Italian legislation, following the European and international guidelines, has increasingly adopted a normative apparatus to ensure proper functioning of the building envelope. The intention is to reduce energy consumption and therefore the environmental impact of buildings during the use phase, which has been proven to be particularly incisive (for instance, the energy consumption of the residential sector for heating and cooling in Italy is 32.2 Mtoe, a measure expressed in tons of oil equivalent) [11]. It is therefore understandable the great effort directed towards the research into construction technologies that can achieve higher energy performance and promote the use of raw materials with lower environmental impact, an interest that has brought back in vogue traditional technological solutions such as the above mentioned earth-based constructions.

Compared to the most common construction solutions, which use reinforced concrete skeletons and poroton envelopes, the raw earth ones, even when stabilised with percentages of Portland cement of around 5%, have an embodied energy of approximately 500 MJ/m^3, which is only equal to 15–25% of the energy incorporated in a conventional brick [9]. Moreover, as we have mentioned, they have excellent thermal dynamic performance, due to their high inertia, with direct consequences for the improvement of thermal comfort in buildings [12].

As is well known, an effective thermal storage mechanism used in construction is based on the latent heat developed by PCM (phase change materials) that accumulate thermal energy at the change of state developed between temperatures of 23 and 20 degrees Celsius: a similar mechanism occurs in the pores of earth-based materials, where thermal energy is used to make the change of state from water to liquid to vapour [13]. In addition to this, it has been shown that, thanks to the good bioclimatic design of a building, the earthen envelopes can lead to the reduction of energy used for heating, cooling, and humidity control [7].

In this paragraph, we will review the main results related to the thermal performance of earthen buildings in different climates and their capability to meet the high standards required by international regulations. This research is based on thermal simulations (1), measurements on a test box (2) and on existing buildings (3). It should be noted that, apart from empirical case studies on existing raw earth buildings, the results obtained from test boxes and thermal simulations tend to return altered results if not based on experimental data [14].

Concerning the first group of publications, these are thermal simulations carried out mainly in Australia, where the construction sector is called to comply with certain requirements established by the National Construction Code (NCC). For 30-cm-thick rammed earth walls (where wet raw earth masses are compacted inside formworks), the minimum thermal resistance required by the NCC impose de facto the addition of thermal insulation to the constructions. Alternatively, in Australia, it is possible to comply with the energy legislation through a rating system, the Star Rating Requirement, which sets limits on energy consumption for heating/cooling depending on the climate zone. This assessment system is used in [7], demonstrating that by varying the type or width of the glazings, their shading system, and the thickness of the walls, the rammed earth building achieves an adequate energy load and can be left uninsulated in areas characterised by semi-arid and Mediterranean climates. Similarly, Hasan and Dutta [15] compare several uninsulated rammed earth construction solutions and show that they are able to meet the annual energy consumption limits in subtropical and tropical climates, while in temperate climates, attention must be paid to the quality of the glazings. Heathcote [16] emphasises that in order to ensure effective cyclical performance for raw earth masonry, thicknesses greater than 45 cm must be adopted to level external summer fluctuations and introduce large glazing in the north (the author works in the southern hemisphere) in order to ensure adequate environmental comfort inside the building during the winter season. A numerical analysis of the summer temperature profile over 24 h was carried out by [17], demonstrating that a 30-cm-thick rammed earth wall can attenuate and stabilise internal temperature fluctuations between 23 and 25 °C. In [18], several upgraded cob wall constructions are compared, using different cavity insulation materials such as paper, straw, or wool; several sustainable earth wall stratigraphies are found, complying with the restrictive UK thermal regulation. The thermal comfort of two sub-Saharan buildings located in Burkina Faso, a traditional adobe and an innovative earthbag one, respectively, are studied in [19]; annual thermal simulations are run in free running conditions, and discomfort hours are studied, revealing that design choices for buildings (shape, location of windows) and the use of typical bioclimatic strategies (roof shading elements, night cross-ventilation) result in enhanced comfort for both types of dwellings.

The second group of publications includes measurements carried out on test boxes. In [20], the thermal performance of the south facades of two rammed earth test boxes, with two different thicknesses, are compared: the first has 50-cm-thick walls and is located in Barcelona, and the second uses 29-cm-thick walls and is located in Lleida. Both test boxes are shown to adequately dampen external temperature fluctuations, but the lower thickness and the more continental climate of the Lleida test box determine a significant difference in terms of the surface temperatures of the walls and the profile of indoor temperatures, producing uncomfortable temperatures in winter. In a later work [21], the authors compare the test box with 29-cm-thick rammed earth walls with a similar one with an extra layer of

internal insulation made of wood fibre: the summer performances of both test boxes, with and without the use of HVAC systems, are assessed and it is confirmed that the addition of the insulation allows a better thermal response to be obtained, reducing the energy consumption for cooling by 45%. Allison et al. [22] collect temperature and humidity data from a test room in England and use this data to confirm, by means of a hygrothermal simulation, the improvement in terms of environmental comfort, air quality, and reduction of energy consumption determined by insulated rammed earth walls.

The latest group of publications include direct measurements of indoor temperatures and humidity in earthen buildings. The above mentioned work by Soudani et al. [12] surveys the thermal performance of a rammed earth building with 50-cm-thick walls located in the region of Isère, France: the house manages to maintain comfortable temperatures both in summer (with maximum indoor temperatures of 28 °C) and in winter (with minimum indoor temperatures around 17 °C, occasionally using a wood-burning stove located in the living room). The importance of associating a correct bioclimatic design strategy with "green" rammed earth buildings is underlined by [23], who analyse a two-storey public building in Australia located in a Mediterranean climate, finding deficiencies in terms of environmental comfort. Krayenhoff [24] lists the positive outcomes of using rigid panel insulation in the rammed earth walls of the SIREWALL constructive system, mainly used in the cold climates of North America; the use of such technology results in mean indoor winter temperatures of 16 °C compared to the 7 °C outside, while humidity is maintained between 40% and 65%, consistent with comfort values. In cold climates, the combined use of thermal insulation (natural or synthetic) and rammed earth walls leads to the amortisation of heating consumption by up to 70%, as reported by [25] with reference to four residential buildings in Canada. Measurements on traditional rammed earth buildings, with 50- to 60-cm-thick rammed earth walls, are made by [26] to measure their real thermal performance. The buildings, heated during the winter period, maintain internal surface temperatures between 15.3 and 16.6 °C, while indoor air temperatures range from 15.7 to 19.4 °C, when outside temperatures are between 3.3 and 1.5 °C. The calculated U-values are between 0.65 and 0.94 W m^2/K, demonstrating the good thermal performance of massive masonry.

The study conducted by [27] illustrates the thermal performance of two identical, uninhabited rammed earth buildings located in Western Australia: one with traditional monolithic rammed earth walls and the other with a polystyrene insulating core. In-situ measurements and simulated thermal behaviours show that the two houses have excellent thermal stability. It is also highlighted how the addition of thermal insulation, in desert climate regions, does not lead to further improvements in thermophysical performance. In [28], the same buildings are studied after the settlement of two families which are consulted about the comfort conditions experienced: the opinions expressed by the inhabitants reflect the good thermal performance of the two buildings which, while requiring occasional use of electric heating in winter, tend to perform very well in summer. The authors conclude that these performances can hardly be described by today's environmental comfort assessment systems used in Australia.

From the presented literature review, it is easy to understand that calibrated thermal simulations must be based on experimental data concerning thermal characterisation of the base raw earth material. As the authors reported in a previous work [29], procedures for the assessment of the thermal properties of raw earth materials are still being developed and nowadays there is no consensus on standard procedures to be used for the evaluation of dry density, thermal conductivity, and specific heat capacity. As many authors point out, thermal measurements should be performed on oven-dried samples (at a temperature of 105°, as in [30–32], or at 50 °C, as in [33]), to determine their water content and assess dry-state thermal properties.

In Table 1 are shown the main contributions to the assessment of the thermal properties of rammed earth materials and the methodologies used. It should be pointed out that the particle size distribution of the soil used and the presence of light aggregates or fibres deeply influence the thermal properties of the final rammed earth material.

Table 1. Thermophysical properties of the rammed earth materials and assessment methods.

Refs.	ρ (kg/m^3)	Assessment Method for ρ	λ (W/m K)	Assessment Method for λ	c_p (J/kg K)	Assessment Method for c_p
[12]	1730	-	0.6 (Sr = 0) 2.4 (Sr = 1)	-	820 (dry) 1158 (wet)	-
[22]	1900	-	0.643	Heat Flow Meter	868	Calculated
[32]	1500–2100	oven-dried samples at T° = 105 °C	0.5228–0.9308	Hot Disk Apparatus	-	-
[34]	1980–2120	oven-dried samples at T° = 105 °C	0.833–1.010 (Sr = 0) 1.369–1.820 (Sr = 1)	Heat Flow Meter	-	-
[35–37]	1340–2080	-	0.19–1.35	Heat Flow Meter	-	-
	2064–2138	-	-	-	1321–1832	Hot guarded plate

In the following paragraphs, the authors present the results of the thermophysical characterisation of an innovative rammed earth material able to reduce the energy demand for cooling space and the improvement of the wellbeing conditions of occupants. The effectiveness of the innovative material was analysed not just through experimental investigation of the material but also through a building energy analysis. Indeed, the energy simulation has been performed with the aim of identifying the best bioclimatic design strategies which include the use of the rammed earth material.

3. Materials and Methods

The methodological approach which is adopted to assess the best design optimisation choices for future Mediterranean rammed earth buildings is organised according to the following steps:

- Thermal characterisation of an optimised local rammed earth material;
- Calibration of thermal and energy simulations on the rammed earth material's properties;
- Search for the optimal design choices for rammed earth buildings in a Mediterranean climate.

The following paragraphs will consider these different aspects in greater depth.

3.1. Thermal Characterisation of the Rammed Earth Material

A dynamic thermal analysis was run to find the optimised design solutions for rammed earth walls in Mediterranean climates. This analysis is based on experimental data acquired to assess the basic thermal properties of an innovative rammed earth material developed in a joint research project with the Guglielmino Soc. Coop., a company working on premixed, natural-based construction materials in Misterbianco, Catania. This innovative material was first developed to gain high mechanical properties, but the chosen stabilisation method enhanced also its final thermal properties. Six mixtures were prepared, using a local inorganic and cohesive soil, a local sand, a filler deriving from another supply chain, natural fibres, and lime. The exact amounts of the components and the methods concerning the sample preparation will be disclosed as soon as the patenting procedure of the final material has been completed.

In this paragraph, we present the methods used to assess the thermal conductivity and the specific heat capacity of the rammed earth reinforced material.

Once samples were prepared, they were immediately removed from the formworks and allowed to dry slowly to avoid cracking in a laboratory where the average temperature and relative humidity during the curing were 20 °C and 60%, respectively. The samples were cured for at least one month.

Once cured, samples were first weighted and then oven-dried at 105 °C, till the differences in two following measurements were lower than 0.1% of the initial weight. After this, we compared the final weight with the initial weight and, if no major differences were registered, we assumed that the dry weight of the material had been calculated and, knowing its volume, the dry density. Samples were then allowed to cool until they reached thermal equilibrium with the laboratory room: temperature equilibrium was assessed by comparing the room temperature with the sample temperature as measured with a needle probe.

Thermal conductivity measurements were carried out on the samples using a ThermTest conductivity meter. The TLS-100 is a handy thermal conductivity meter which measures thermal conductivity and thermal resistivity. Transient Line Source (TLS) is based on the ASTM D5334 standard. The sensor needle comprises a thin heating wire and temperature probe enclosed in a 50-mm steel tube. The sensor must be entirely introduced into the sample to be tested: this meant that the samples needed to be drilled and cleared from dust and powder; then, in order to minimise any contact resistance between the sensor needle and the sample, a thermal paste of $\lambda > 4$ m^{-1} K^{-1} was applied on the TLS-100 needle (a 5-cm-long and 5-mm-thick needle, ideal for material of higher density). Once the needle was inserted, the sample was heated by a constant current source and the temperature increment was registered over a defined period. Temperature increment was plotted against the logarithm of time, and the slope of this curve was used for the calculation of thermal conductivity λ.

The specific heat capacity tests were performed on representative crushed samples of the six fibre-reinforced rammed earth batches. Measurements were performed with a Shimadzu DSC-60 device for the calorimetric characterisation. Enthalpy and temperature calibrations of the apparatus were made according to manufacturer's specifications, using as standard materials indium (NIST SRM 2232), tin (NIST SRM 2220), and zinc (NIST SRM 2221a) for temperature; indium (NIST SRM 2232) for heat flow. Samples were first placed in sealed aluminium crucibles. Then, a heating rate of 10 °C min^{-1} was selected for measurements. Differential scanning calorimetry (DSC) scans were carried out from room temperature to 300 °C. Once DSC curves were obtained, we converted heat flux to specific heat capacity through (1), considering a Δ T of ten degrees.

$$Q = m \times c_p \times \Delta T \qquad (1)$$

3.2. Thermal Inertia and Dynamic Parameters

Since the introduction of a new constructive technology must be supported by effective convenience of its adoption, a careful analysis must be carried out in order to assess its possibility of improvement compared to conventional building technologies, concerning the reduced environmental impact (in production, construction, use, and dismission phases), its indoor thermal comfort, its increased structural and energetic performances, and economic accessibility.

Thermal loads of a building and consequently its indoor thermal comfort are strongly dependent on the building's thermal inertia, which is a passive method to store heat energy and to delay its restitution [38–40]. The thermal inertia of the building envelope depends on the thermal properties of materials [39–41]. However, other parameters that may affect the thermal inertia of the building are the air change rate, the orientation of the building, and internal gains [41–44].

The higher the thermal inertia of a building, the slower the rate at which its indoor air temperature rises and drops [39]. The propagation of temperature profiles on the wall exposed to cyclical solar radiation and variable outdoor air temperature is assumed to be sinusoidal.

In the passage from outdoor to indoor surface of the wall, the sinusoidal temperature wave reduces its amplitude gradually [39,45,46]. This phenomenon is associated with the thermal mass of building components and analysed through two dynamic parameters, the time lag (TL) and the decrement factor (DF) [42,45,47].

Time lag (TL) is defined as the time required for a temperature wave to be transferred from the outer surface of the wall to its inner surface [45,47] and is expressed as follows:

$$TL = \tau_{T_{si,max}} - \tau_{T_{so,max}} \tag{2}$$

where τ is time, in s; T_{si} is inner surface temperature, in °C; T_{so} is outer surface temperature, in °C.

The decrement factor (DF) is defined as the ratio between the amplitude of inner surface temperature fluctuation and that of outer surface temperature fluctuation [45].

$$DF = \frac{A_{si}}{A_{so}} = \frac{T_{si,max} - T_{si,min}}{T_{so,max} - T_{so,min}} \tag{3}$$

where A_{si} is the amplitude of the heat wave on the inner surface, in °C; A_{so} is the amplitude of the heat wave on the outer surface, in °C.

3.3. Thermal and Energy Analysis

As many authors point out [48–51], the thermal performance of buildings and the influences of thermal mass and passive strategies can be assessed only through dynamic thermal simulations. Consequently, the detailed dynamic thermal behaviour of a representative rammed earth building in compliance with the in-force building regulation standard was analysed.

Design Builder Version 6.0 [52], based on the Energy Plus calculation engine, was used to carry out the dynamic simulations of the selected building.

Different configurations of the simulated building model have been proposed to investigate the effects of different bioclimatic strategies (summer night cross-ventilation, use of overhangs, and combined effects). Analysed scenarios are Base, Base + N.V.50, Base + Over, and Base + N.V.50 + Over, respectively.

The thermal analysis was performed considering two operating regimes, i.e., in free-running conditions and in the presence of an air conditioning system, respectively. Therefore, two cycles of annual simulation referring to the year 2019 were carried out using a calculation frequency of 12 time steps per hour.

Under free-running conditions, an assessment of the thermal response of massive rammed earth envelopes to outer forcing conditions and an evaluation of the thermal comfort in indoor spaces were carried out in the summer period. The indoor and outdoor superficial temperature profiles of the walls facing east and west were determined in order to calculate the time lag and decrement factor according to Equations (2) and (3).

The indoor thermal comfort was assessed by means of the adaptive model considering categories I, II, and III, according to the standard UNI EN 15251: 2008 [53]. The percentages of the analysed period in which the indoor operative temperature of the investigated scenarios allow comfort conditions (within categories I, II, and III, respectively) to be calculated.

In the presence of the air conditioning system, the specific cooling energy needs per year were calculated considering the building equipped with the air conditioning system to maintain a temperature of 26 °C during the cooling season in indoor spaces. Proposed configurations were compared in terms of normalised cooling energy saving with respect to the cooling energy needs of the basic model (Base).

Furthermore, an optimisation analysis has been run to efficiently search and identify the design options for the constructions to best meet key design performance objectives. Design Builder Optimisation works using genetic algorithms (GA) to search for optimal design solutions, in a trade-off analysis on different design variables aiming at two objectives: the best design options are the ones which combine the minimum values for the two objectives, outlining a Pareto Front along the bottom-left part of the data point cloud graph.

3.4. Energy Saving

The energy saving derived by the adoption of proposed interventions is calculated for each i-th scenario through the difference among the cooling energy needs of the base case $(PE_C)_{Bs}$ and cooling energy of the current scenario $(PE_C)_i$:

$$(ES_C)_i = (PE_C)_{BS} - (PE_C)_i \qquad (4)$$

Moreover, with the aim of comparing the different scenarios, the energy savings for space cooling $(ES_C)_i$ are normalised with respect to the value of the baseline scenario $(PE_C)_{BS}$:

$$(ES_C)_i = \frac{(PE_C)_{BS} - (PE_C)_i}{(PE_C)_{BS}} \qquad (5)$$

where $(PE_C)_{BS}$ is the absolute maximum value of energy demand for space cooling of the building; i-th = 1, −4 are the possible design configurations (Base, Base + N.V.50, Base + Over, Base + N.V.50 + Over).

4. Investigation

4.1. Definition of a Representative Rammed Earth Building: Geometry and Technology

The base design of the case study has been developed on the basis of the Peruvian Standard NTE E.080 [54]. In order to comply with this earthquake-resistant raw earth constructions standard, raw earth walls must be at least 40-cm-thick, to counter the risk of overturning; moreover, they must be equipped with horizontal (floors and roofs) and vertical (buttresses and transverse walls) stiffening elements; finally, the density of the walls in the two main directions must be homogeneous.

The seismic design criteria of this standard are based on resistance, stability, and performance. The resistance criterion concerns the horizontal action exerted by the earthquake on the walls, which causes shear and bending on the walls parallel and perpendicular to the direction of the earthquake, respectively. The stability criterion refers to the limits of thickness, vertical and horizontal slenderness of the walls, size, and location of voids. Finally, the performance criterion, together with the two mentioned above, requires that effective reinforcement systems are put in place to control movement during the earthquake.

The designed rammed earth residential building consists of a rectangular box, with three rooms on the south exposition and two rooms on the sides. All loadbearing rammed earth walls are 40 cm thick, while partitions are made with lightweight materials. Geometrical features of the building are reported in Table 2.

Table 2. Geometrical data of the rammed earth case study building.

Building Characteristics	h (m)	Total Envelope Surface (m²)	Total Gross Volume (m³)	Shape Factor (1/m)	Net Floor Area (m²)	Glazing Area (m²)	Glazing Surface/ Total Envelope Surface (-)
	3.3	825.9	261.4	3.16	58.92	4.9	0.0059

The basic constructions used for the building components, their thermal transmittance, and superficial mass values are shown in Table 3. Concerning the rammed earth walls, they were first considered uninsulated to investigate the single effect of using thick earth walls with higher thermal inertia. The thermophysical properties of the implemented constructions were deduced by archival data, except for the experimental campaign carried out on the innovative rammed earth material used for wallings.

Table 3. Basic constructions of the building components.

Ground Solid Floor (U = 0.347 W/m² K, Ms = 1743.45 kg/m²)

Layer	Material	t (m)	ρ (kg/m³)	c_p (J/kg K)	λ (W/m K)	R (m² K/W)	Ms (kg/m²)
	Interior					0.170	
1	Timber Flooring	0.01	650	1200	0.14	0.071	6.5
2	Polyethylene	0.003	980	1800	0.5	0.005	2.45
3	Cork Board	0.05	160	1890	0.04	1.250	8
4	Fibreboard	0.015	300	1000	0.06	0.250	4.5
5	Dry Sand	0.08	1700	1000	0.6	0.133	136
6	Fibreboard	0.02	300	1000	0.06	0.333	6
7	Air Layer Unventilated floor	0.15				0.210	
8	Reinforced Concrete	0.6	2300	1000	2.3	0.210	1380
9	Cast Concrete	0.1	2000	1000	1.13	0.210	200
	Exterior					0.040	

Roof (U = 0.332 W/m² K, Ms = 81.4 kg/m²)

Layer	Material	t (m)	ρ (kg/m³)	c_p (J/kg K)	λ (W/m K)	R (m² K/W)	Ms (kg/m²)
	Interior					0.100	
1	Fibreboard	0.015	300	1000	0.06	0.250	4.5
2	Cork Board	0.07	160	1890	0.04	1.750	11.2
3	Fibreboard	0.015	300	1000	0.06	0.250	4.5
4	Cavity Unventilated	0.05				0.180	
5	Fibreboard	0.02	300	100	0.06	0.333	6
6	Asphalt Roll Roofing	0.002				0.027	
7	Loose Fill Powder Gravel	0.03	1840	840	0.36	0.083	55.2
	Exterior					0.040	

Wall (U = 1.15 W/m² K, Ms = 412.25 kg/m²)

Layer	Material	t (m)	ρ (kg/m³)	c_p (J/kg K)	λ (W/m K)	R (m² K/W)	Ms (kg/m²)
	Interior					0.130	
1	Lime Sand Render	0.025	650	1200	0.8	0.031	16.25
2	Rammed Earth Wall	0.4	1980	1800	0.628	0.637	392
3	Gypsum Plaster Mortar	0.025	160	1890	0.8	0.031	4
	Exterior					0.040	

Windows are realised with a 5-cm oak wood frame and a double 6-mm glazing and 13-mm air gap. The overall thermal transmittance value of the windows is 3.00 W/m² K, and the solar heat gain coefficient (glass g-value) is 0.75.

4.2. Building Simulation Model and Settings

In the Design Builder model, all rooms of the reference residential building were considered as occupied zones. The internal loads are characterised by occupants, electrical devices, and cooking and lighting systems for a total of 928 W with a density of 16 W/m². The power density of occupancy is 7.00 W/m² for a crowding of 0.05 people/m²; the power density of electrical devices and lighting are 5.00 and 4.00 W/m², respectively. The same internal heat loads are fixed for all the proposed configurations of simulations.

For infiltration of outdoor air, a constant of air change of 0.5 vol/h was set up.

Under the AC system scenario, the building is equipped with a heat pump (HP) system that supplies both heating and cooling. A HP system with a coefficient of performance (SCOP = 3.50) and energy efficiency ratio (EER = 2.50) when it operates as chiller was used. The calculation of the overall thermal energy needs of building was carried out considering
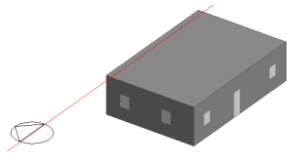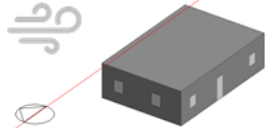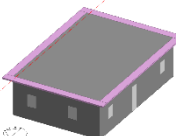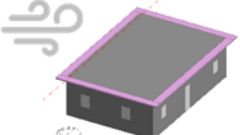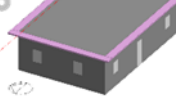
two operation programs as established by Italian laws [55] for heating and cooling season, respectively. The conditioning system operates with a set-point temperature of 20 °C during heating season and 26 °C in cooling season.

The meteorological data of the Energy Plus Weather (EPW) file for the city of Catania updated to the year 2019 were used as weather input for dynamic thermal simulations.

4.3. Investigated Models

Different scenarios of the analysed building model were set in Design Builder in order to assess the single effect of every optimised strategy (both bioclimatic and constructive). A basic model (Base) was first developed to investigate the effect of highly massive material for vertical envelopes, as rammed earth is. Design optimisation choices were first made applying different traditional bioclimatic strategies to the base model, and then comparing different insulated solutions for the walls using the Optimisation Design Builder tool, which allow for comparison of different variables (in this case, the external wall constructions) against two main objectives (i.e., minimisation of energy needs, capital costs, embodied carbon, and discomfort hours). Starting from the results of the annual dynamic simulations, it was possible to assess the optimised design solutions to obtain optimal thermal stability to ensure a satisfactory level of comfort and minimise energy needs, costs, and environmental impact. The different simulation cases are codified and described in Table 4.

Table 4. Codification for the simulated cases.

Code	Building Model	Description of Case
Base		Base model: uninsulated rammed earth walls, insulated roof and ground solid floor. No natural ventilation, no overhang solutions for shadings
Base + N.V. 50		Base model + natural ventilation by the 50% opening of windows
Base + Over		Base model with 60-cm overhangs
Base + N.V. 50 + Over		Base model with 60-cm overhangs + natural ventilation by the 50% opening of windows
Opt + N.V. 50 + Over		Optimised insulated models (comparison of 31 insulated constructions) with 60-cm overhangs + natural ventilation by the 50% opening of windows

For the sake of brevity, the authors extrapolated and analysed the thermal behaviour of the rammed earth building in a representative summer period (28 July–2 August) to study the best design options to be applied on massive earth walls in a hot temperate climate as the Mediterranean one.

4.4. Use of Night Cross-Ventilation

Use of natural night cross-ventilation has been considered in the Base + N.V. 50 coded analysis. In this configuration, 50% of the glazed surface in the building was kept open from 00:00 a.m. to 06:00 a.m. according to a specific schedule in order to investigate the effectiveness of night-time natural ventilation [55–57].

4.5. Use of Overhangs

In Base + Over coded analysis, a 60-cm-deep coronation of the roof was used to analyse their shadowing effects on walls. These overhangs, inherited by traditional Mediterranean bioclimatic strategies and typically used in contemporary rammed earth constructions (the "great hat" which raw earth buildings must be provided with [58]), were implemented as an independent component in Design Builder. An equivalent conductivity of 0.043 W/mK for this component was set.

4.6. Combined Effects

The coded analysis Base + N.V. 50 + Over shows the combination effects of the night cross-ventilation (at 50% of windows opening) and use of overhangs.

4.7. Use of Wall Thermal Insulation

The last part of the analysis (Opt + N.V. 50 + Over) is a set of five optimisation simulations, focusing on the use of several types of thermal wall insulation aiming at minimising costs, embodied carbon, and discomfort hours in the building, while minimising energy needs for heating and cooling. The optimised constructions for the earth walls consist of the use of thirty-one combinations of internal or external thermal insulation, all resulting in a final thermal transmittance below 0.43 W/m^{2}K, which is the limit value of Italian standard regulations for climate zone B (in which the city of Catania is located) [59–61]. The main thermal and physical characteristics of these types of insulation are reported in Table 5.

Table 5. Type and thermophysical properties of the insulation used in the optimised cases.

Type of Insulation	ρ (kg/m^3)	c (J/kgK)	λ (W/m^{2}K)	Origin
Expanded Polystyrene EPS board	15	1400	0.04	Synthetic
Polyurethane PU board	35	1590	0.028	Synthetic
Aerogel	150	1000	0.015	Synthetic
Rockwool	100	710	0.033	Mineral
Glasscellular sheet	140	840	0.048	Mineral
Perlite	65	840	0.046	Mineral
Rubber	1200	1000	0.15	Composite
Cork board	160	1890	0.04	Vegetal
Jute felt mat	330	1090	0.067	Vegetal
Coconut fibre board	520	1090	0.06	Vegetal
Flax shive board	500	1880	0.012	Vegetal
Thermal plaster hemp lime	400	1500	0.085	Vegetal
Recycled vegetal fibreboard	290	1300	0.055	Vegetal
Straw	310	1300	0.057	Vegetal
Sheepwool mat	18	1720	0.037	Animal

5. Results and Discussion

5.1. Experimental Results on Rammed Earth Material

The basic thermal properties and the dry density of the rammed earth mixtures are shown in Table 6. In the following thermal analysis, we worked with mix F (Figure 1).

Table 6. Thermophysical properties of the rammed earth materials developed with the Guglielmino Soc. Coop.

Mix	Type of Components	ρ (kg/m³)	λ (W/m K)	c_p (J/kg K)	a (m²/s)
A	Soil, Sand	2055	0.605	1045	3.0466×10^{-7}
B	Soil, Sand, Fibre	1944	0.619	1760	1.7812×10^{-7}
C	Soil, Sand, Lime	1939	0.532	907	3.0842×10^{-7}
D	Soil, Sand, Filler	2043	0.721	690	5.1592×10^{-7}
E	Soil, Sand, Filler, Lime	1870	0.521	1430	1.9852×10^{-7}
F	Soil, Sand, Filler, Fibre	1990	0.628	757	4.2411×10^{-7}

Figure 1. (**a**) Rammed earth samples; (**b**) Thermal conductivity measurements.

5.2. Thermal Behaviour of External Walls

The thermal behaviour of a non-conditioned building is strongly affected by the façade orientation, as well as the thermal inertia properties of its envelope components. For the sake of brevity, considering that the façades facing east and west have rather similar behaviour, especially with respect to midday, only the hourly profile of the surface temperatures of the wall facing east during period (28 July–2 August) is shown in Figure 2. Afterwards, the maximum and minimum values of inner and outer surface temperatures of the west-oriented wall are reported next to values of the surface temperatures of the façade facing east in Table 7.
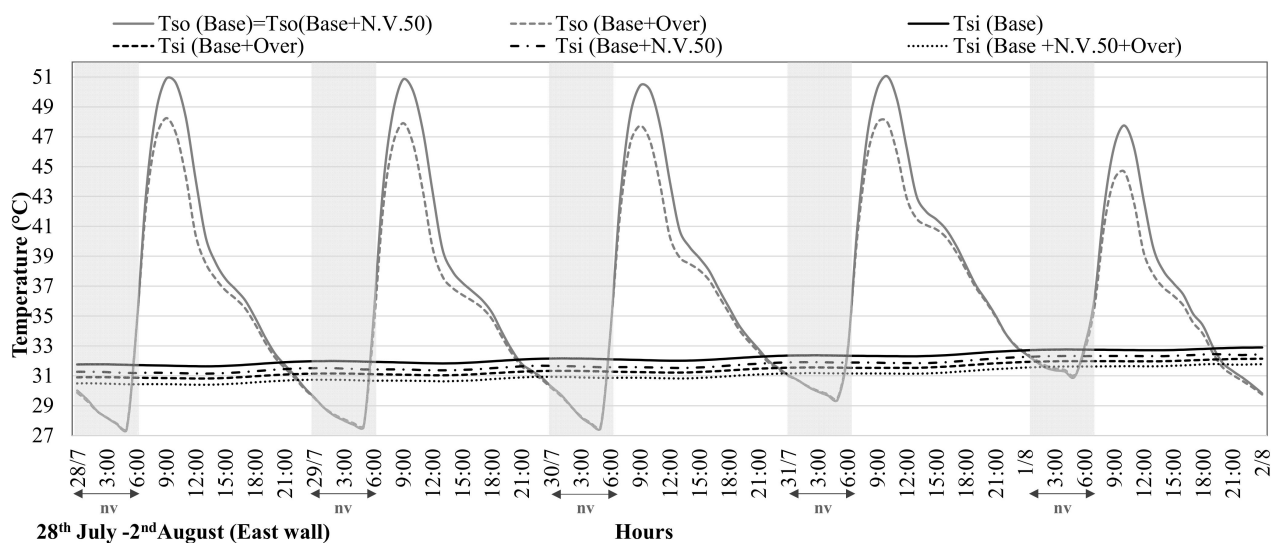

Figure 2. Outdoor surface temperature (T_{se}) vs. indoor surface temperature (T_{si}) in the investigated cases from 28 July to 2 August.

Table 7. Thermal inertia of the envelope in the studied cases for east and west exposure.

Scenario °C	East Wall						West Wall					
	$T_{so,max}$	$T_{so,min}$	$T_{si,max}$	$T_{si,min}$	$\Delta T_{so,max}$	$\Delta T_{si,max}$	$T_{so,max}$	$T_{so,min}$	$T_{si,max}$	$T_{si,min}$	$\Delta T_{so,max}$	$\Delta T_{si,max}$
Base	51.1	27.50	32.76	31.8	23.33	0.16	49.92	27.89	32.9	31.5	21.33	0.71
Base + N.V.50	51.1	27.41	32.33	31.4	23.37	0.10	49.87	27.83	32.5	30.8	21.32	0.79
Base + Over	48.3	27.59	31.99	31.0	20.57	0.12	47.64	27.96	32.4	30.9	18.45	0.72
Base + N.V.50 + Over	48.1	27.54	31.64	30.7	20.49	0.08	47.59	27.88	32.0	30.3	18.49	0.76

Figure 2 depicts the hourly variation in inner surface temperature (T_{si}) and outer surface temperature (T_{so}) of the wall facing east for all investigated configurations. Under the base case, the hourly path-line of T_{si} ranges from a minimum of 31.8 °C to a maximum of 33 °C considering the entire selected period against a variation in T_{so} from a minimum of 27.8 °C to a maximum of 51.0 °C.

It should be highlighted that the inner surface temperature is kept almost constant with respect to the curve of outer surface temperature in all investigated scenarios. The daily amplitude of the trend of T_{si} is, on average, 1.0 °C, which is very small if compared to that of T_{so}. This behaviour is confirmed by a very low value of decrement factor, DF = 0.0045 and DF = 0.0253, for walls facing east and west. The peak of T_{si} is delayed by 17 h with respect to the maximum value of T_{so}. This reveals that the fibre-reinforced rammed earth walls behave as a thermal flywheel and remarkably dampen the incoming heat wave.

Under the night-time natural ventilation scenario (Base + N.V.50), the trend of T_{si} is approximately 0.4 °C lower than that of the base case.

The addition of the overhangs to the base case (Base + Over) produces a decrease of 3 °C in the peak values in the outer surface temperature. Against the decrement in the maximum value of T_{so}, a reduction in the inner surface temperature of 0.8 °C for the wall facing east and 0.5 °C for the wall facing west were obtained during the analysed period.

The best results are achieved under the combined effects of night ventilation and overhangs (Base + N.V.50 + Over). Combined strategies succeed in lowering indoor surface temperatures by more than 1.0 °C, in the maximum and minimum values of T_{si} both on east and west walls, the bioclimatic strategies using overhangs being more effective compared to that using only night ventilation.

Table 7 summarises the main results of all scenarios for east and west exposure.

Indoor surface temperatures decrease less in upgrading interventions using night cross-ventilation, while the use of overhangs has significant consequences for the reduction of indoor surface temperatures.

The analysis of the thermal dynamic responses of the wall facing west leads to analogous considerations of those observed for the wall facing east. It has to be highlighted that, as a result of the orientation of the building, the west wall shows a peak in indoor surface temperature the next day with respect to the action of external forcing agents (T_o and solar radiation).

Figure 3 displays the thermal dynamic parameters calculated for the walls facing east and west.
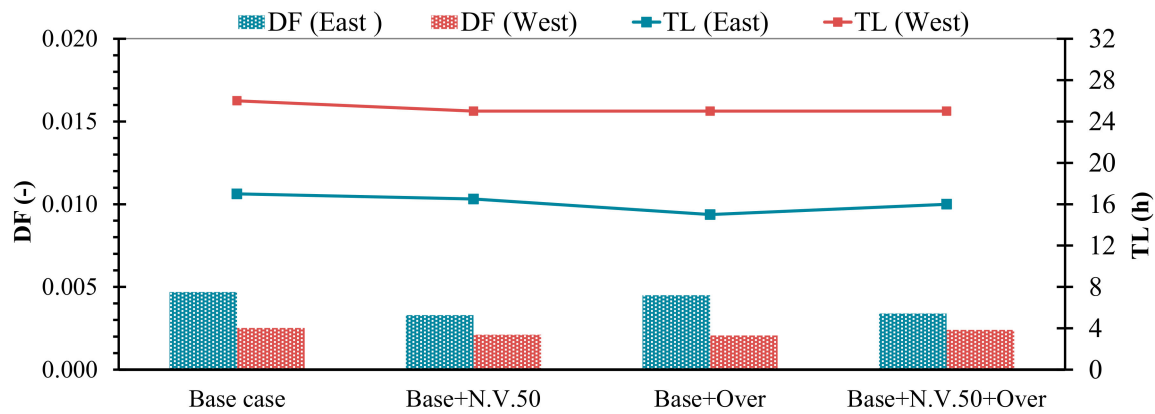
Figure 3. Decrement factor (DF) and time lag (TL) of east- and west-facing walls.

It has to be highlighted that the basic configuration shows appreciable thermal dynamic behaviour, TL = 17 h, DF = 0.0045 for the east wall and TL = 26 h, DF = 0.00253 for the west wall. Comparing the TL and DF values of the investigated cases, it can be observed that time lag remains almost constant in the various upgrading scenarios, while the decrement factor tends to decrease in combined and more complex design solutions.

5.3. Assessment of Indoor Thermal Comfort

An evaluation of the thermal conditions in indoor spaces under the investigated scenarios was conducted analysing the trend of indoor air temperature. In the presence of internal heat gains, the hourly profile of air temperature from 28 July and 2 August is plotted in Figure 4. A double bedroom and a single bedroom were selected as the investigated rooms.
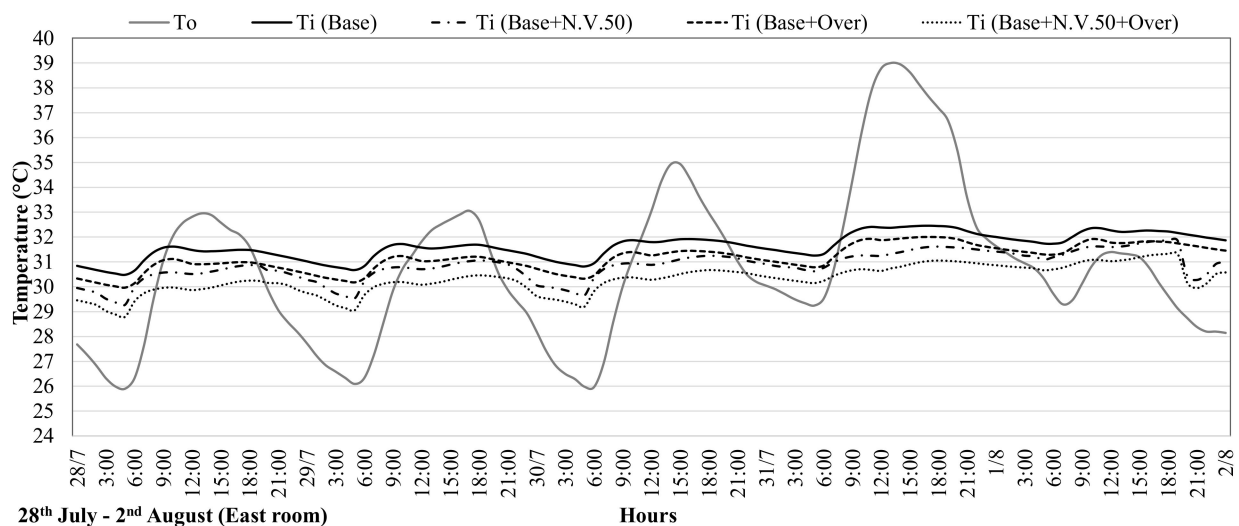
Figure 4. Hourly profiles of indoor air temperature (Ti) in the investigated cases from 28 July to 2 August.

In the base case, the air temperature (Ta) ranges from a minimum of 31.8 °C at 6.00 a.m. to a maximum of 33.5 °C at 12.00 a.m. The effect of night natural ventilation reduces the peak of Ta by approximately 0.80 °C in the Base + N.V. 50 scenario, as shown in Figure 4.

The overhang (Base + Over) scenario shows an average reduction of 0.50 °C with respect to the trend in air temperature of the base case. Consequently, the use of night cross-ventilation is more effective compared to the use of overhangs under indoor air temperature.

With reference to the base case, the reductions in air temperature in the different scenarios are shown in Table 8. The best configuration is the combined strategy (Base +

N.V. 50 + Over), which succeeds in lowering the maximum temperatures by 1.40 °C for the east room and 1.51 °C for the west room, while the minimum temperatures are reduced by 1.68 °C in the east room and 1.92 °C in the east room, during the same day.

Table 8. Mean indoor temperature for the investigated cases for east and west rooms.

Scenario °C	East Room				West Room			
	$T_{a,max}$	$T_{a,min}$	$\Delta T_{a,max}$	$\Delta T_{a,min}$	$T_{a,max}$	$T_{a,min}$	$\Delta T_{a,max}$	$\Delta T_{a,min}$
Base	32.46	30.48	-	-	32.66	30.25	-	-
Base + N.V.50	31.61	29.28	0.84	1.20	31.79	28.71	0.99	1.54
Base + Over	32.00	29.97	0.45	0.51	32.35	29.78	0.43	0.47
Base + N.V.50 + Over	31.05	28.80	1.40	1.68	31.27	28.34	1.51	1.92

It should be highlighted that the reductions in the minimum values of air temperature are higher than those in the maximum values of air temperature.

The indoor thermal comfort of the building was evaluated according to the approach of the adaptive comfort model. The operative temperature (T_{op}), calculated under free-running condition for the entire year and for all investigated cases, was used as the reference parameter for assessing the indoor thermal comfort. The hourly variations in T_{op} during the selected period (28 July to 2 August) are depicted in Figure 5 as well as the range of the comfort temperatures for categories I, II, and III.
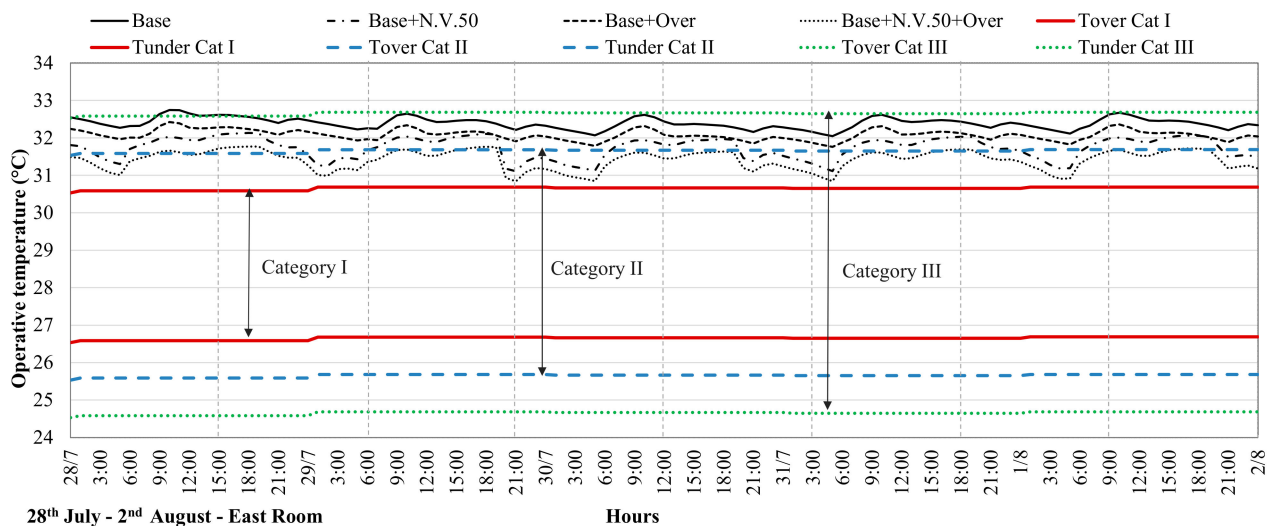

Figure 5. Hourly profile of operative temperature under all investigated cases and threshold values (T under, T over) for category I, II, and III.

Under the base scenario, the profiles of the operative temperature (T_{op}) range from a minimum value of 32.0 °C to a maximum value of 32.7 °C. Under the overhang scenario (Base + Over), the path-line of T_{op} is reduced by approximately 0.5 °C with respect to the base case during the entire investigated period. Both the Base and Base + Over cases show moderate comfort levels because their profiles of T_{op} are predominantly within category III. In the Base + N.V. 50 scenario, the profile of operative temperature lies in category III during the hottest hours, whereas its profile is within category II in early morning.

It is interesting to point out that the use of simple bioclimatic combined strategies (use of night cross-ventilation and overhangs in the case Base + N.V. 50 + Over) allows a further

improvement in the trend of operative temperature. The decrease in T_{op} allows for the passage from a moderate level of comfort to a normal expected one, yet not satisfying the limits for the more restrictive category I for the eastern room (double bedroom), while in the western room (single bedroom), they are satisfied in early morning.

Table 9 summarises the percentages of the analysed period (28th July to 2nd August) in which the investigated scenarios are within the comfort categories I, II, and III, respectively.

Table 9. Percentage time during 28 July–2 August in which the investigated cases are in comfort categories I, II, and III for double bedroom (east room) and single bedroom (west room).

Cases (%)	East Room				West Room			
	Base	**Base + N.V. 50**	**Base + Over**	**Base + N.V. 50 + Over**	**Base**	**Base + N.V. 50**	**Base + Over**	**Base + N.V. 50 + Over**
Cat. I	0	0	0	0	0	5.79	0	12.50
Cat. II	0	35.54	0	80.99	22.31	66.94	52.07	75.21
Cat. III	91.73	64.46	100	19.01	72.72	27.27	47.93	12.30
Out Cat. III	8.26	0	0	0	5.79	0	0	0

As can be observed, for the east and west rooms, the Base case lies for most of the time (respectively, 91.73% and 72.72%) within category III of comfort, with the west room being more comfortable during early morning, when it satisfies category II for 22.31% of the time. The Base + N.V.50 design solution allows for a consistent passage to higher comfort categories, both for the east (35.54% in category II) and west rooms (66.94% in category II and 5.79% in category I), compared to the use of overhangs, which provides only a moderate improvement in indoor thermal comfort. Finally, combined strategies (Base + N.V.50 + Over) enhance overall comfort in all rooms, with major percentages in category II (80.99% for east room and 75.21% for west room) and minor percentages in category III (east and west rooms) and category I (west room).

5.4. Cooling Energy Needs

The comparison among the different proposed investigated cases was also carried out in terms of cooling energy needs. The cooling energy needs are calculated considering the cooling system being switched on during the selected period for Catania according to Italian Standard Regulations.

The base case is characterised by specific annual energy needs equal to 86.1 kWh/m^{2}y and needs for cooling are 34.3 kWh/m^{2}y. The calculated energy needs, as well as the energy savings, for the base configuration and for the upgraded ones, are depicted in Figure 6.
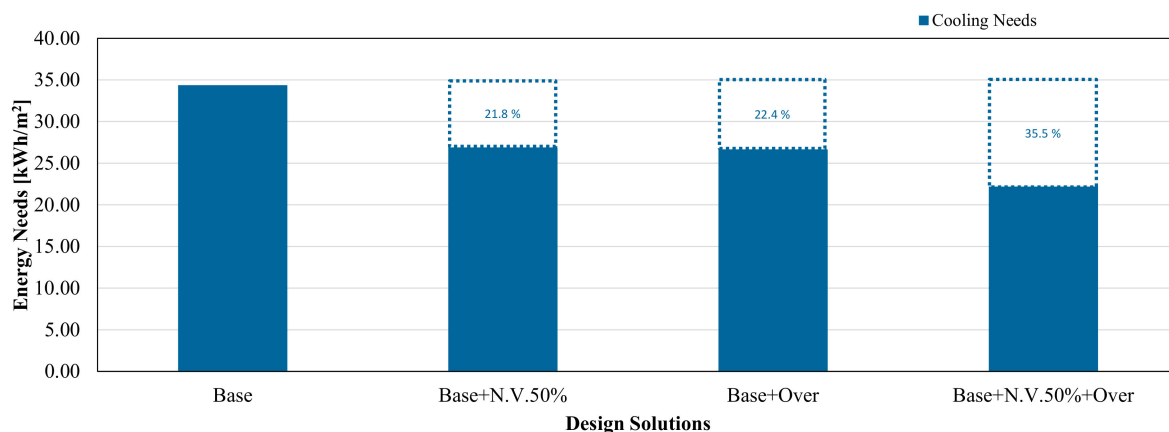

Figure 6. Cooling energy needs for all the investigated cases.

It should be highlighted that the Base + Over and the Base + N.V. 50 scenarios show an energy saving of around 22% if compared to the Base case. The results highlight that the use of combined bioclimatic strategies (for the case Base + N.V. 50 + Over) allow a remarkable improvement to be achieved in the energy performance of the whole building. The cooling energy needs are reduced from 34.30 kWh/m^2 to a value of 22.1 kWh/m^2 when the Base + N.V. 50 + Over case is applied. Therefore, an energy saving of 35.5% can be achieved in the cooling season.

5.5. Potentiality of the Multicriteria Optimisation for Rammed Earth Solid Walls

In the last section of this investigation, on the basis of the best bioclimatic strategy option (Base + N.V. 50 + Over), thirty-one design solutions for the vertical envelope were studied. The intention of this analysis was to best identify the design approach that must be adopted for massive rammed earth walls to be used in Mediterranean climates. The idea of using thermal insulation was not so obvious for a hot temperate climate as the one in Catania, as it might have caused indoor overheating. Moreover, several considerations had to be made before choosing a compatible type of thermal insulation for a sustainable, affordable, and low-embodied-energy building material such as rammed earth.

As mentioned above, the Design Builder Optimisation tool was used to plot the design solutions for rammed earth wall constructions, which minimised the heating and cooling loads against three other objectives, aiming at minimising total building cost, embodied carbon, and discomfort hours. Design Builder offered a wide database concerning embodied carbon and costs for all the materials implemented. Results are depicted in Figures 7 and 8. For the sake of brevity, it is shown only one of the analyses aiming at the minimisation of discomfort hours (the one fitting category II).
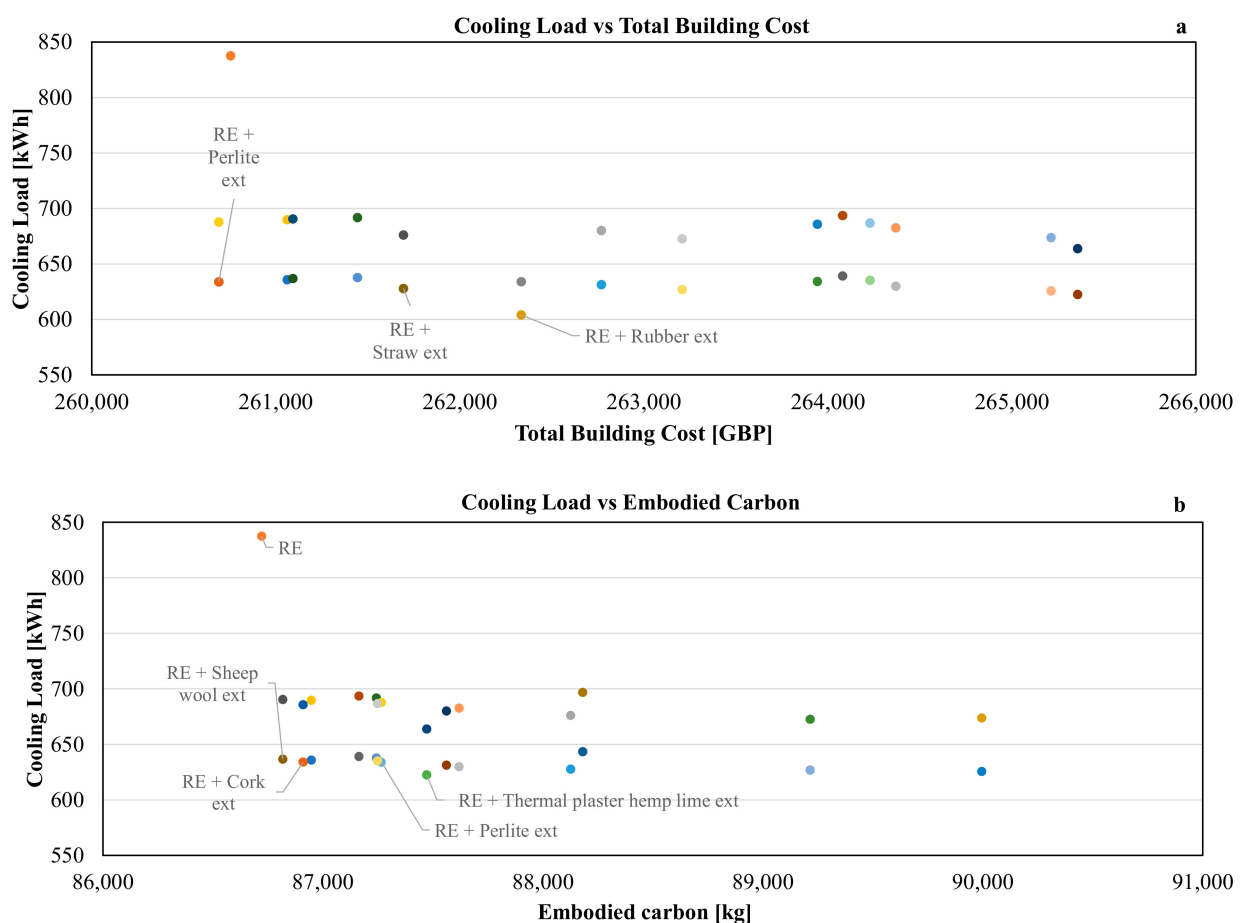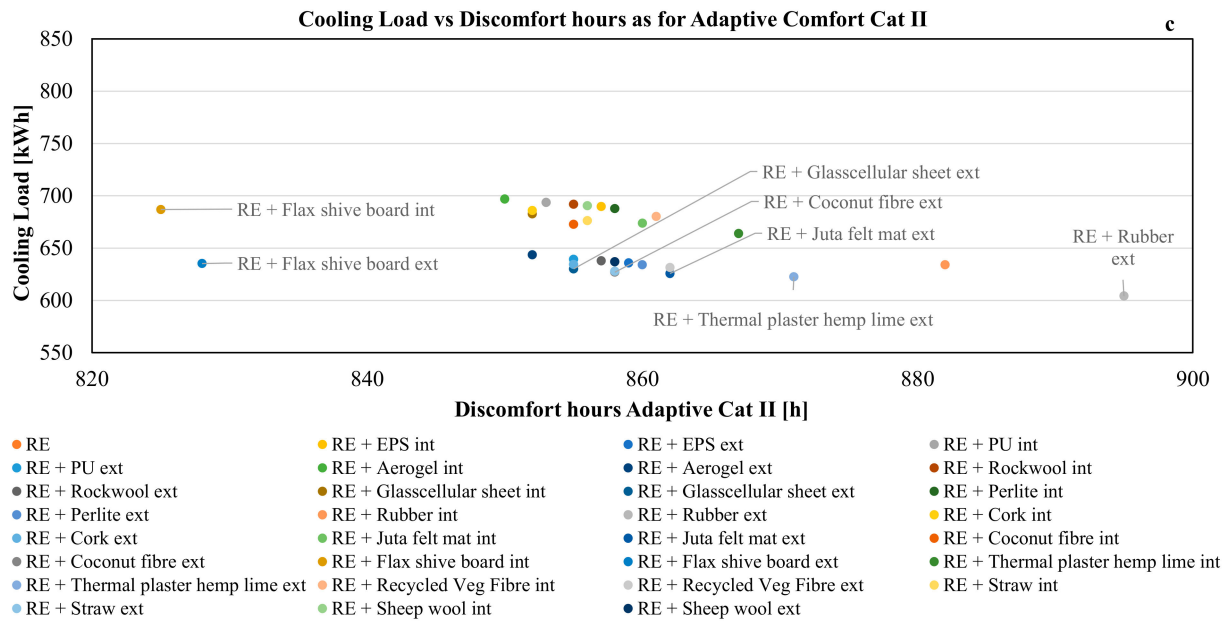

Figure 7. *Cont.*

Figure 7. Cooling loads vs. total building cost (**a**), embodied carbon (**b**), and discomfort hours as for category II of adaptive comfort model (**c**). Optimised rammed earth (RE) insulated wall constructions indicated with labels.
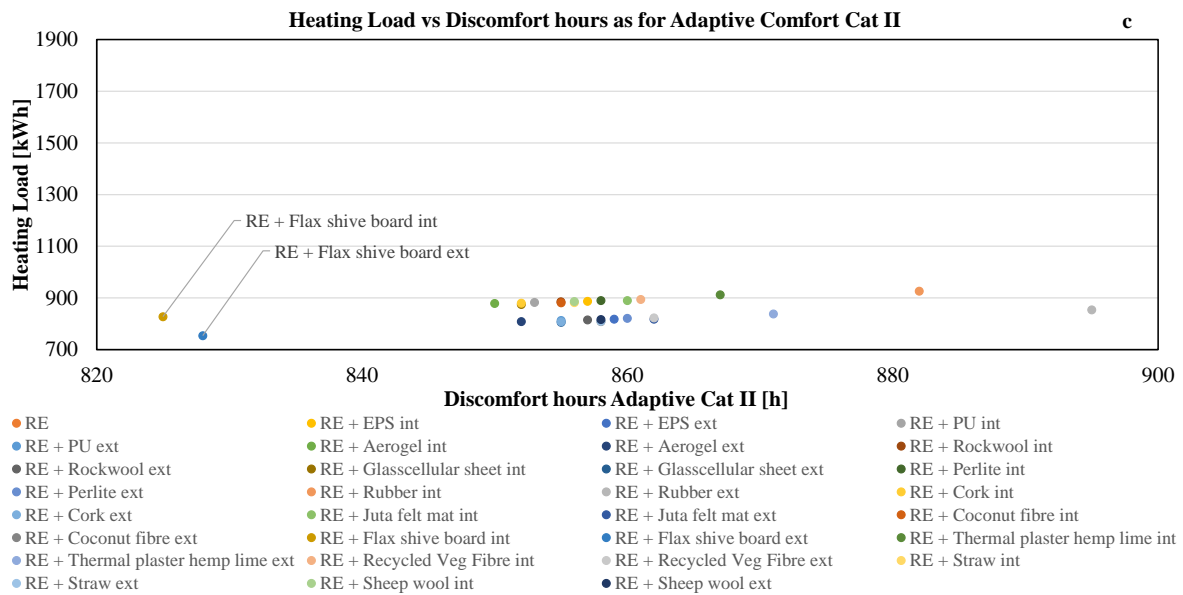

Figure 8. *Cont.*

Figure 8. Heating loads vs. total building cost (**a**), embodied carbon (**b**), and discomfort hours as for category II of adaptive comfort model (**c**). Optimised rammed earth (RE) insulated wall constructions indicated with labels.

Concerning the minimisation of cooling load, the minimum cost is found for both conventional insulation types (such as perlite and hard rubber external insulation) and natural-based ones (straw). At the same time, some conventional insulation types (such as perlite and hard rubber) and other natural-based insulation types such as thermocork boards, sheepwool mats, and thermal plaster realised in lime hemp, together with the uninsulated rammed earth (RE) construction, are the best options to achieve the objective of the minimisation of embodied carbon. Finally, the objective of the minimisation of discomfort hours is satisfied by several insulated construction solutions, most of them using innovative natural-based insulation (10-cm jute felt, 9-cm-thick coconut fibreboard, 2-cm-thick flax shive board, and 12-cm thermal hemp lime plaster), and only two using conventional synthetic insulation (glasscellular and hard rubber). It should be noted that the uninsulated solution lies outside the range presented in Figure 8c, as the annual discomfort hours are 1099. The great presence of optimised solutions using natural-based thermal insulation is remarkable, especially when compared to the low presence of synthetic and composite materials.

A similar result is also visible when minimisation of heating load is taken into account: in this case, some synthetic insulating materials (EPS and rockwool), mineral (perlite), and natural-based ones (thermocork, coconut fibre and flax shive boards, straw, and sheepwool mat) satisfy also the minimisation of total building cost. Concerning the minimisation of embodied carbon, the uninsulated rammed earth solution, together with flax shive board and sheepwool mat, meet also the minimisation of heating loads. Finally, the best design solutions minimising both heating loads and discomfort hours are the ones encountering the use of flax shive board insulation; the uninsulated solution is not an optimised one concerning comfort, its annual discomfort hours being superior to the shown range. It is interesting to point out that some conventional insulation types used by several Australian and North American rammed earth construction firms, such as polyurethane and expanded polystyrene boards, do not satisfy the economic, environmental, and comfort criteria in the analysed Mediterranean climate. Indeed, similar results are encouraging for the upcoming generation of natural-based thermal insulation, even when applied to rammed earth construction.

6. Conclusions

This contribution focused on the use of passive design strategies to improve indoor thermal comfort and energy needs in rammed earth dwellings to be used in Mediterranean

climates. A representative rammed earth residential building located in Catania (Italy) has been designed on the basis of the Peruvian Standard NTE E.080, which regulates the design of reinforced and seismic-resistant raw earth buildings. Its thermal behaviour in free-running conditions and energy performances have been simulated with Design Builder software. The model was calibrated using weather data implemented by the research group in 2019. Thermophysical performance of the innovative fibre-reinforced rammed earth material has been assessed in the laboratory of the University of Catania and implemented in the Design Builder model.

The research shows the effects of different design solutions inherited by traditional Mediterranean bioclimatic strategies, as the use of massive walls with high thermal inertia, use of night cross-ventilation, overhangs, and a combination of the strategies. The effectiveness of the use of bioclimatic approaches was proven by the assessment of inner surface temperature, indoor mean air temperature, comfort expectations, and energy needs for cooling. Furthermore, in the last part of the paper, we explored the potentiality of using multicriteria analysis to design the optimal thermal insulation for rammed earth walls in hot temperate climates. The key findings of this study can be summarised as follows:

- The development of an innovative rammed earth material with combined stabilisation strategies (fibres and filler) resulted in a material with lower thermal conductivity and satisfactory specific heat capacity, compared to conventional rammed earth values;
- The use of a massive material as rammed earth for the envelope keeps the curve of inner surface temperature almost constant with respect to the curve of outer surface temperature, with low values of decrement factor (DF < 0.005 for east wall and west wall) and satisfactory values of time lag (TL > 17 h for east and west wall);
- Indoor mean air temperature profile for the best bioclimatic design option (Base + Over + N.V.50 scenario) lies between 28.3 and 31.27 °C in the analysed period, with a significative reduction compared to the base model;
- The innovative fibre-reinforced rammed earth walls behave as a thermal flywheel and remarkably dampen the incoming heat wave;
- Combined bioclimatic strategies (Base + Over + N.V.50 scenario) succeed in satisfying normal comfort expectations for uninsulated rammed earth walls without use of HVAC systems in summer conditions, for more than 75% of the analysed time;
- Concerning energy needs for space cooling, the use of combined bioclimatic strategies (Base + Over + N.V.50 scenario) reduces energy demand for cooling by 35.5% with respect to the base case.

The need to further minimise energy consumption led us to consider the use of a thermal insulation layer to be applied on the rammed earth walls.

The last part of the paper focuses on the potentiality of using multicriteria analysis to design the optimal thermal insulation for rammed earth walls in hot temperate climates. The Optimisation Design Builder tool was used to find the design options for wall constructions (with a choice between 31 stratigraphies) which could, at the same time, minimise energy consumption, costs, environmental impact, and discomfort. Interesting outputs of this analysis are:

- The identification of several optimised solutions using an external layer of natural-based thermal insulation (as jute felt mats, coconut fibre and flax shive boards, and thermal hemp lime plaster);
- An additional reduction in discomfort hours of around 20% for the abovementioned optimised insulated constructions;
- A further decrease in energy needs for cooling by 25% for the abovementioned optimised insulation options;
- The exclusion of several synthetic insulation types (EPS, PU boards) conventionally used in Australian and American rammed earth construction, for the optimised solutions in Mediterranean climates.

For the outlined reasons, it is understood that design optimisation strategies must start with a good bioclimatic design, which is made specific to the dwelling site by collecting data via secular research regarding the adaptation to local climatic and geographic conditions, and then transitioning to the optimisation of all the building components and the materials used.

Choices concerning thermal insulation should be made considering the real economic and environmental prices of these products, which strongly depend on the geographical context where the building will be located, and carefully selecting the products which can positively affect indoor comfort and energy consumption.

Finally, as some of the optimised construction solutions depicted in this study require the use of natural-based thermal insulation, future works must focus on the influence of water vapour's contribution to energy and the thermal and physical behaviour of rammed earth walls, especially when considering the durability properties of these constructions using natural-based materials.

References

1. *Report WWF "Cambiamenti Climatici, Ambiente ed Energia"*; WWF Italia Ong-Onlus: Roma, Italy, 2009; Available online: http://www.climatrentino.it/binary/pat_climaticamente/cc_clima_mitigazione/Mitigazione_Line_guida_WWF.1326206502.pdf (accessed on 1 December 2020).
2. Available online: https://ec.europa.eu/clima/policies/strategies/2030_en (accessed on 1 December 2020).
3. Hoornweg, D.; Bhada-Tata, P. *What a Waste: A Global Review of Solid Waste Management*; Urban Development & Local Government Unit, World Bank: Washington, WI, USA, 2012.
4. Available online: https://www.iea.org/reports/tracking-buildings/building-envelopes#abstract (accessed on 1 December 2020).
5. Bollini, G. Terra Battuta: Tecnica Costruttiva e Recupero. In *Linee Guida per le Procedure di Intervento*; Edicom Edizioni: Milano, Italy, 2013.
6. Hickson, P. Earth Building how does it rate. In *AA.VV. Rammed Earth Construction*; Ciancio & Beckett, Taylor & Francis Group: London, UK, 2015.
7. Dong, X.; Soebarto, V.; Griffith, M. Strategies for reducing heating and cooling loads of uninsulated rammed earth wall houses. *Energy Build.* **2014**, *77*, 323–331. [CrossRef]
8. Giuffrida, G.; Caponetto, R.; Cuomo, M. An overview on contemporary rammed earth buildings: Technological advances in production, construction and material characterization. *IOP Conf. Ser. Earth Environ. Sci.* **2019**, *296*, 012018. [CrossRef]
9. Venkatarama Reddy, B.V.; Prasanna Kumar, P. Embodied energy in cement stabilised rammed earth walls. *Energy Build.* **2010**, *42*, 380–385. [CrossRef]
10. Arrigoni, A.; Beckett, C.; Ciancio, D.; Dotelli, G. Life cycle analysis of environmental impact vs. durability of stabilised rammed earth. *Constr. Build. Mat.* **2017**, *142*, 128–136. [CrossRef]
11. *Energy Efficiency Annual Report 2018*; ENEA: Rome, Italy, 2018.
12. Soudani, L.; Woloszyn, M.; Fabbri, A.; Morel, J.C.; Grillet, A.C. Energy evaluation of rammed earth walls using long term in-situ Measurements. *Sol. Energy* **2017**, *141*, 70–80. [CrossRef]

13. Fabbri, A.; Morel, J.C. Earthen materials and constructions. In *AA. VV. Nonconventional and Vernacular Construction Materials, Woodhead Publishing Series in Civil and Structural Engineering*; Woodhead Publishing: Cambridge, UK, 2013.

14. Soudani, L.; Fabbri, A.; Chabriac, P.A.; Morel, J.C.; Woloszyn, M.; Grillet, A.C. On the relevance of neglecting the mass vapor variation for modelling the hygrothermal behaviour of rammed earth. In *AA.VV. Rammed Earth Construction*; Ciancio & Beckett, Taylor & Francis Group: London, UK, 2015.

15. Hasan, M.M.; Dutta, K. Investigation of energy performance of a rammed earth built commercial office building in three different climate zones of Australia. In *AA.VV. Rammed Earth Construction*; Ciancio & Beckett, Taylor & Francis Group: London, UK, 2015.

16. Heathcote, S. The thermal performance of earth buildings. *Inf. Construcción* **2011**, *63*, 117–126. [CrossRef]

17. Stone, C.; Katunsky, D. Dynamic Thermal Properties of Uninsulated Rammed Earth Envelopes. *Int. J. Eng. Inf. Sci.* **2015**, *10*, 103–112.

18. Goodhew, S.; Griffiths, R. Sustainable earth walls to meet the building regulations. *Energy Build.* **2005**, *37*, 451–459. [CrossRef]

19. Rincón, L.; Carrobé, A.; Martorell, I.; Medrano, M. Improving thermal comfort of earthen dwellings in sub-Saharan Africa with passive design. *J. Build. Eng.* **2019**, *24*, 100732. [CrossRef]

20. Rincón, L.; Serrano, S.; Cabeza, L.F.; Ganzález, B.; Navarro, A.; Bosch, M. Experimental rammed earth prototypes in Mediterranean climate. In *AA.VV. Earthen Architecture: Past, Present and Future*; Mileto, C., Vegas, F., García Soriano, L., Cristini, V., Eds.; Taylor & Francis Group: London, UK, 2015.

21. Serrano, S.; De Gracia, A.; Cabeza, L.F. Adaptation of rammed earth to modern construction systems: Comparative study of thermal behaviour under summer conditions. *Appl. Energy* **2016**, *175*, 180–188. [CrossRef]

22. Allinson, D.; Hall, M. Hygrothermal analysis of a stabilised rammed earth test building in the UK. *Energy Build.* **2010**, *42*, 845–852. [CrossRef]

23. Taylor, P.; Fuller, R.J.; Luther, M.B. Energy use and thermal comfort in a rammed earth office building. *Energy Build.* **2008**, *40*, 793–800. [CrossRef]

24. Krayenhoff, M. Rammed Earth Thermodynamics. In *AA.VV. Rammed Earth Construction*; Ciancio, D., Beckett, C.T.S., Eds.; Taylor & Francis Group: London, UK, 2015.

25. MacDougall, C.; Dick, K.J.; Krahn, T.J.; Wong, T.; Cook, S.; Allen, M.; Leskien, G. Thermal performance summary of four rammed earth walls in Canadian climates. In *AA.VV. Rammed Earth Construction*; Ciancio & Beckett, Taylor & Francis Group: London, UK, 2015.

26. Lovec, V.B.; Jovanović-Popović, M.D.; Živković, B.D. Analysis of heat transfer coefficient of rammed earth wall in traditional houses in Vojvodina. *Therm. Sci.* **2017**, *21*, 2919–2930. [CrossRef]

27. Beckett, C.T.S.; Cardell-Oliver, R.; Ciancio, D.; Huebner, C. Measured and simulated thermal behaviour in rammed earth houses in a hot-arid climate. Part A: Structural behaviour. *J. Build. Eng.* **2018**, *15*, 243–251. [CrossRef]

28. Beckett, C.T.S.; Cardell-Oliver, R.; Ciancio, D.; Huebner, C. Measured and simulated thermal behaviour in rammed earth houses in a hot-arid climate. Part B: Comfort. *J. Build. Eng.* **2017**, *13*, 146–158. [CrossRef]

29. Giuffrida, G.; Caponetto, R.; Nocera, F. Hygrothermal properties of raw earth materials: A literature review. *Sustainability* **2019**, *11*, 5342.

30. Moevus, M.; Anger, R.; Fontaine, L. Hygro-thermo-mechanical properties of earthen materials for construction: A literature review. In Proceedings of the TERRA 2012, 12th Siacot Proceedings, 11th International Conference on the Study and Conservation of Earthen Architectural Heritage, 12th Iberian-American Seminar on Earthen Architecture and Construction, Lima, Peru, 22–27 April 2012.

31. Ashour, T.; Korjenic, A.; Korjenic, S.; Wu, W. Thermal conductivity of unfired earth bricks reinforced by agricultural wastes with cement and gypsum. *Energy Build.* **2015**, *104*, 139–146. [CrossRef]

32. Zhang, L.; Yang, L.; Petter Jelle, B.; Wang, Y.; Gustavsen, A. Hygrothermal properties of compressed earthen bricks. *Constr. Build. Mat.* **2018**, *162*, 576–583. [CrossRef]

33. Cagnon, H.; Aubert, J.E.; Coutand, M.; Magniont, C. Hygrothermal properties of earth bricks. *Energy Build.* **2014**, *80*, 208–217. [CrossRef]

34. Hall, M.; Allinson, D. Analysis of the hygrothermal functional properties of stabilised rammed earth materials. *Build. Environ.* **2009**, *44*, 1935–1942. [CrossRef]

35. Barbeta Solà, G.; Massó Ros, F.X. Improved thermal capacity of rammed earth by the inclusion of natural fibres. In *Rammed Earth Construction*; Beckett, C., Ed.; Taylor Francis Group: London, UK, 2015.

36. Barbeta Solà, G.; Massó Ros, F.X. Thermal improvement of rammed earth buildings by the inclusion of natural cork. In *Earthen Architecture: Past, Present and Future*; Mileto, C., Vegas, F., Cristini, G.S., Eds.; Taylor Francis Group: London, UK, 2015.

37. Porter, H.; Blake, J.; Dhami, N.K.; Mukherjee, A. Rammed Earth blocks with improved multifunctional performance. *Cem. Concr. Compos.* **2018**, *92*, 36–46. [CrossRef]

38. Ulgen, K. Experimental and theoretical investigation of effects of wall's thermophysical properties on time lag and decrement factor. *Energy Build.* **2002**, *34*, 273–280. [CrossRef]

39. Ozel, M.; Pihtili, K. Optimum location and distribution of insulation layers on building walls with various orientations. *Build. Environ.* **2007**, *42*, 3051–3059. [CrossRef]

40. Xing, J.; Xiaosong, Z.; Yiran, C.; Geng, W. Thermal performance evaluation of the wall using heat flux time lag and decrement factor. *Energy Build.* **2012**, *47*, 369–374.

41. Gagliano, A.; Patania, F.; Nocera, F.; Signorello, C. Assessment of the dynamic thermal performance of massive buildings. *Energy Build.* **2014**, *72*, 361–370. [CrossRef]
42. Stephan, E.; Cantin, R.; Caucheteux, A.; Tasca-Guernouti, S.; Michel, P. Experimental assessment of thermal inertia in insulated and noninsulated old limestone buildings. *Build. Environ.* **2014**, *80*, 241–248. [CrossRef]
43. Roucoult, J.M.; Douzane, O.; Langlet, T. Incorporation of thermal inertia in the aim of installing a natural nighttime ventilation system in buildings. *Energy Build.* **1999**, *29*, 129–133. [CrossRef]
44. Orosa, J.A.; Oliveira, A.C. A field study on building inertia and its effects on indoor thermal environment. *Renew. Energy* **2012**, *37*, 89–96. [CrossRef]
45. Asan, H.; Sancaktar, Y.S. Effects of wall's thermophysical properties on time lag and decrement factor. *Energy Build.* **1998**, *28*, 159–166. [CrossRef]
46. Aste, N.; Angelotti, A.; Buzzetti, M. The influence of external walls thermal inertia on the energy performance of well insulated buildings. *Energy Build.* **2009**, *41*, 1181–1187. [CrossRef]
47. Duffin, R.J. A passive wall design to minimize building temperature swings. *Solar Energy* **1984**, *33*, 337–342. [CrossRef]
48. Ascione, F.; De Rossi, F.; Vanoli, G.P. Energy retrofit of historical buildings: Theoretical and experimental investigations for the modelling of reliable performance scenarios. *Energy Build.* **2011**, *43*, 1925–1936. [CrossRef]
49. Cornaro, C.; Puggioni, V.A.; Strollo, R.M. Dynamic simulation and on-site measurements for energy retrofit of complex historic buildings: Villa Mondragone case study. *J. Build. Eng.* **2016**, *6*, 17–28. [CrossRef]
50. Gagliano, A.; Nocera, F.; Patania, F.; Moschella, A.; Detommaso, M.; Evola, G. Synergic effects of thermal mass and natural ventilation on the thermal behaviour of traditional massive buildings. *Int. J. Sustain. Energy* **2016**, *35*, 411–428. [CrossRef]
51. Nocera, F.; Caponetto, R.; Giuffrida, G.; Detommaso, M. Energetic Retrofit Strategies for Traditional Sicilian Wine Cellars: A Case Study. *Energies* **2020**, *13*, 3237. [CrossRef]
52. Design Builder. "Energy Simulation Software." Version 6. 2019. Available online: http://designbuilder.co.uk (accessed on 1 December 2020).
53. *European Standard EN 15251:2007 Indoor Environmental Input Parameters for Design and Assessment of Energy Performance of Buildings Addressing Indoor Air Quality, Thermal Environment, Lighting and Acoustics*; European Committee for Standardization: Brussels, Belgium, 2007.
54. Norma, E.080 Diseño y Construccion Con Tierra Reforzada, Ministerio de Vivienda, Construcción y Saneamiento, El Peruano. Lima. 2017. Available online: https://www.sencico.gob.pe/descargar.php?idFile=3478 (accessed on 1 December 2020).
55. Evola, G.; Marletta, L.; Natarajan, S.; Patanè, E. Thermal inertia of heavyweight traditional buildings: Experimental measurements and simulated scenarios. *Energy Procedia* **2017**, *133*, 42–52. [CrossRef]
56. Giuffrida, S.; Ventura, V.; Nocera, F.; Trovato, M.R.; Gagliano, F. Technological, axiological and praxeological coordination in the energy-environmental equalization of the strategic old town renovation programs. In *Green Energy Technology*; Springer: Berlin, Germany, 2020; pp. 425–446.
57. Nocera, F.; Faro, A.L.; Costanzo, V.; Raciti, C. Daylight performance of classrooms in a mediterranean school heritage building. *Sustainability* **2018**, *10*, 3705. [CrossRef]
58. Houben, H.; Guillaud, H. *CRATerre: Traité de Construction en Terre*; Éditions Parenthèses: Marseille, France, 2006.
59. *Decreto Interministeriale 26 Giugno 2015, Adeguamento Linee Guida Nazionali per la Certificazione Energetica degli Edifici*. 2015. Available online: https://www.gazzettaufficiale.it/eli/id/2015/07/15/15A05198/sg (accessed on 1 December 2020).
60. Fernandez-Antolin, M.-M.; del Río, J.M.; Costanzo, V.; Nocera, F.; Gonzalez-Lezcano, R.-A. Passive design strategies for residential buildings in different Spanish climate zones. *Sustainability* **2019**, *11*, 4816. [CrossRef]
61. Gagliano, A.; Detommaso, M.; Nocera, F.; Patania, F.; Aneli, S. The retrofit of existing buildings through the exploitation of the green roofs—A simulation study. *Energy Procedia* **2014**, *62*, 52–61. [CrossRef]